ACS Photonics

Article

pubs.acs.org/journal/apchd5

Photonic Structure Textile Design for Localized Thermal Cooling Based on a Fiber Blending Scheme

Peter B. Catrysse,* Alex Y. Song, and Shanhui Fan

Edward L. Ginzton Laboratory and Department of Electrical Engineering, Stanford University, Stanford, California 94305, United States

ABSTRACT: There is great potential for energy savings in buildings if temperature set points of cooling systems can be extended by 1−2 °C (2−4 °F) provided that the thermal comfort of building occupants is maintained. Since most body heat is dissipated through thermal radiation, the photonic properties of textiles can play an essential role in localized thermal cooling. Current textiles are very opaque at infrared wavelengths and prevent the efficient transmission of thermal radiation from the human body when temperature set points are increased. In this work, we show a design approach for photonic structure textiles based on fiber materials that are both comfortable to wear and allow localized thermal cooling at increased set points. Our design principle is based on the blending of fibers that are largely infrared transparent to achieve efficient cooling and natural, infrared-opaque fibers for comfort of wearing. We use a full-vector electromagnetic field method to calculate our designs' spectral, directional properties and we apply a detailed radiative heat transfer model based on a full spectral, directional net radiation method that we developed. We demonstrate that our designs, containing up to one-third cotton and two-thirds nylon, allow net heat transfer at an extended set point of 26.1 °C (79 °F) that exceeds the cooling abilities of a cotton-only design at the current thermal comfort set point of 23.9 °C (75 °F), which can result in more than 30% energy savings. We also find that the combined (radiative, convective and conductive) heat transfer for our designs at 26.1 °C (79 °F) exceeds the metabolic power rate of 58.2 W/m^2 for an adult in a sedentary state.

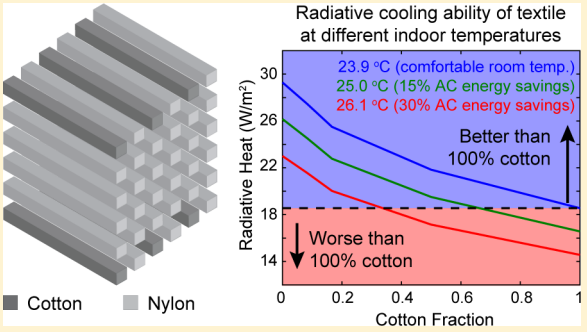

KEYWORDS: *photonic structure textiles, thermal radiation engineering, localized thermal management, radiative cooling, natural textile fiber materials, infrared transparent textile fiber materials*

Energy usage by the buildings sector (residential and commercial) dominates at 40.2% the primary energy consumption in the United States.[1] Space heating and cooling account for one-third of the energy consumed in the buildings sector and amount to 13.4% of all energy used domestically.[1] Reducing energy demand for heating and cooling can thus have an important impact on electricity usage, fuel consumption, and greenhouse gas emissions.[2]

The primary reason for space cooling and heating is to maintain the thermal comfort of the building occupants.[3] The building heating, ventilation, and air conditioning (HVAC) system creates comfortable thermal conditions for most occupants when the temperature set points are 21.1 °C (70 °F) for heating and 23.9 °C (75 °F) for cooling.[4] When the temperature is in the neutral-band between these set points, the building HVAC system takes no action. Expanding set points by 2.2 °C (4 °F) in each direction, that is, creating a wider neutral-band, can generate energy savings of 15−60% depending on location and climate.[4]

Maintaining the thermal comfort for building occupants in this scenario requires thermal management. Local thermal management solutions (LTMS) are particularly attractive. The ability to control the exchange of thermal energy near the body (at the local level) rather than at the room level can leverage the large difference in thermal envelope size between a typical room and its occupants.[5] Passive LTMS for cooling and heating in conjunction with set point expansion therefore offer great potential for energy savings. Unfortunately, they have as yet to deliver.[6] Localized cooling, in particular, is a challenging problem.

Thermal radiation plays a major role in the dissipation of heat generated by the human body. Studies have shown that radiative heat transfer contributes to more than 50% of total body heat loss in an office situation.[7−9] Improving heat transfer through thermal radiation is thus essential in localized thermal management for cooling. Recent studies have shown that passive radiative cooling requires the understanding and engineering of photonic properties.[10−14] In this work, the photonic properties of textiles are important. Typical clothing is made from conventional textiles that consist of natural fibers, such as cotton or linen, or synthetic fibers, such as polyester. These fibers are largely opaque in the thermal infrared (IR) wavelength range, that is, they exhibit low IR transmissivity.[15] Consequently, they prevent body heat from radiating out efficiently when the temperature set point of the room is increased above the typical comfort range 21.1−23.9 °C

Received: August 26, 2016

DOI: 10.1021/acsphotonics.6b00644
ACS Photonics XXXX, XXX, XXX−XXX

(70−75 °F). One can certainly imagine textile designs that efficiently transmit the thermal radiation emitted by the skin using fiber materials that are inherently transparent in the IR wavelength range[16,17] or even designs that blend synthetic fibers.[16] For comfort of wearing, however, one would like to be able to use a wider range of textile fiber materials. Natural fibers, in particular, are most comfortable to wear, although they are not IR transparent. Hence, one needs to devise a method for designing thermally transparent textiles that incorporate natural fiber materials, such as cotton or wool, while retaining the IR transparency required for cooling LTMS, as well as preserve the opacity of the textiles at visible wavelengths.

RESULTS AND DISCUSSION

Our Approach: Incorporate Natural Fibers while Retaining IR Transparency. Our goal is to design photonic structure textiles that are both IR transparent and offer the comfort of wearing of a conventional textile with natural fibers. Our design principle for achieving these photonic structure textiles, unlike blending of several synthetic fibers,[16] is to use a fiber blending scheme that includes both fibers that are largely transparent in the IR thermal wavelength range, and natural fibers that are comfortable to wear but opaque to thermal radiation. We can thus create textile designs that enable the control of thermal radiation for cooling at the clothing level, yet provide the comfort of wearing to which we are accustomed.

Fibers used in conventional textiles, including natural fibers, exhibit large absorption in the thermal IR range resulting from vibrational modes of the molecular bonds inside the fiber materials. The absorption peaks associated with these modes, for example, C−O stretching (7.7−10 μm), C−N stretching (8.2−9.8 μm), aromatic C−H bending (7.8−14.5 μm), S═O stretching (9.4−9.8 μm),[18,19] overlap in wavelength range with the peak thermal radiation from the human body (9.4 μm for skin at 33.9 °C). With an IR absorptivity ∼0.7 or more,[20] cotton and wool-based textiles, for example, are IR opaque and largely prevent body heat from radiating out efficiently.

There exist fiber materials for which the absorption peaks do not overlap spectrally with the thermal radiation generated by the human body. Examples of such IR transparent fibers, which are compatible with textile production, include polyethylene and nylon. Polyethylene (PE) only has C−H and C−C bonds with strong absorption peaks at 3.4, 3.5, 6.8, and 13.7 μm,[21] which are all far away from human body radiation. Nylon contains an additional amide group which has vibrational modes in the 6−8 and 13−18 μm wavelength ranges.[22]

In this paper, we show how to tailor the optical properties of textiles using photonic structures to enable radiation control at the clothing level and provide localized cooling capabilities. Specifically, we demonstrate designs that incorporate natural (IR opaque) fibers for comfort of wearing, preserve textile opacity in the visible wavelength range, and exhibit increased IR transmissivity so that the temperature set point in an office environment can be extended from 23.9 (75) to 26.1 °C (79 °F) without affecting comfort.

Electromagnetic Calculations: Full Spectral, Directional Properties. First, we demonstrate that the optical properties of photonic structure textile designs, which contain both natural fibers and IR transparent fibers, can be tailored to obtain IR transparency with a significant fraction of natural fibers for comfort of wearing, while retaining opacity of the textile in the visible wavelength range. To show thermal and visible radiation control with such photonic structure textiles, we analyze their optical properties in the thermal IR wavelength range (7−18 μm), which includes the peak wavelength of thermal radiation from the skin, and in the visible wavelength range (400−700 nm). As a textile model, we consider a multilayered periodic array of parallel fibers (Figure 1) with

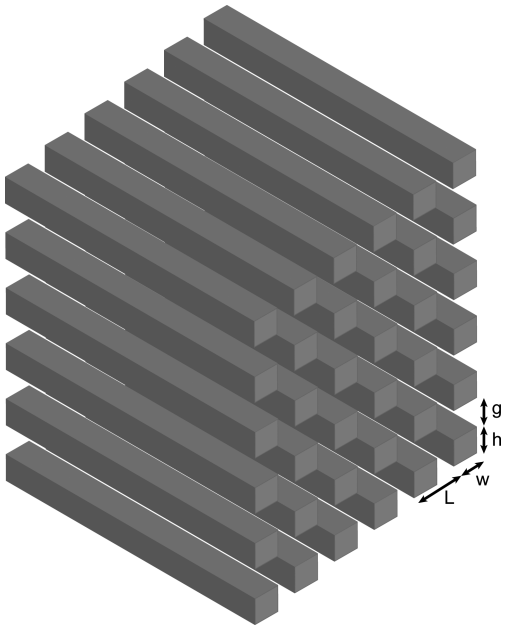

Figure 1. Textile geometry consisting of a multilayered periodic array of parallel fibers. The fiber arrays have a periodicity L. The individual fibers have a square cross-section with side $w = h$. The array layers are separated by a distance g.

square cross-section ($w = h$), periodicity (L), and gap/separation between layers (g). The fiber size, periodicity, and the number of layers are based on values from literature and are chosen to achieve IR opacity in conventional textiles.[16,23]

We compare the spectral, directional transmissivity, reflectivity, and absorptivity of three textile designs: a conventional textile design based on cotton (IR opaque) fibers, a textile made purely of nylon (IR transparent) fibers, and an IR transparent design based on a fiber blending scheme with cotton and nylon. We use cotton since it is a textile material that is appreciated for its comfort of wearing. For transparency in the thermal wavelength range, we use nylon as IR transparent material since it has a very small extinction coefficient in the thermal range for typical office temperatures. Moreover, nylon fibers are compatible with current textile technologies.

We assume an example textile design structure with six layers of parallel fibers (Figure 2). The fiber size is $w = 4.25$ μm and the array periodicity is $L = 5$ μm. Individual fiber layers are separated by a distance $g = 0.75$ μm. In the conventional design, all six layers consist of a periodic array of parallel cotton fibers (Figure 2a). Figure 2c shows a design based on nylon fibers only. The geometry and dimensions remain otherwise unchanged. In the IR transparent textile based on our design approach (Figure 2b), we have blended nylon and cotton fibers. In this example, the nylon fibers are added to the inner layers for increased transparency, while the external (top and bottom) layers contain cotton fibers for comfort of wearing.

DOI: 10.1021/acsphotonics.6b00644
ACS Photonics XXXX, XXX, XXX−XXX

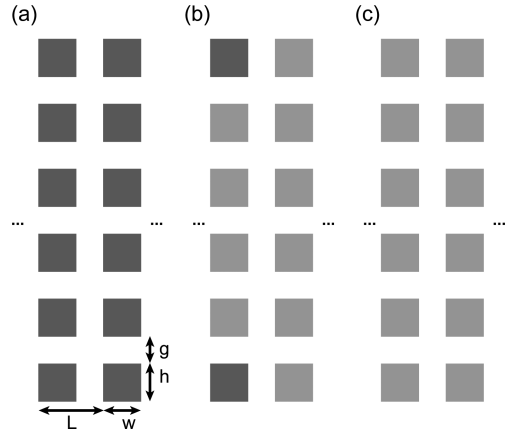

Figure 2. Example textile design based on a six-layer structure. (a, c) Conventional textile design based on periodic arrays of parallel cotton fibers (dark gray) and textile design based on periodic arrays of IR transparent nylon fibers (light gray). (b) IR transparent textile design based on a fiber blending scheme with cotton fibers on external layers for wearing comfort and nylon fibers on internal layers for increased IR transparency. The arrays have a periodicity $L = 5\ \mu$m. The fibers have a square cross-section with side $w = 4.25\ \mu$m. The array layers are separated by a distance $g = 0.75\ \mu$m.

Figure 3 shows the transmission spectra in the IR thermal wavelength range between 7 and 18 μm for normal incidence

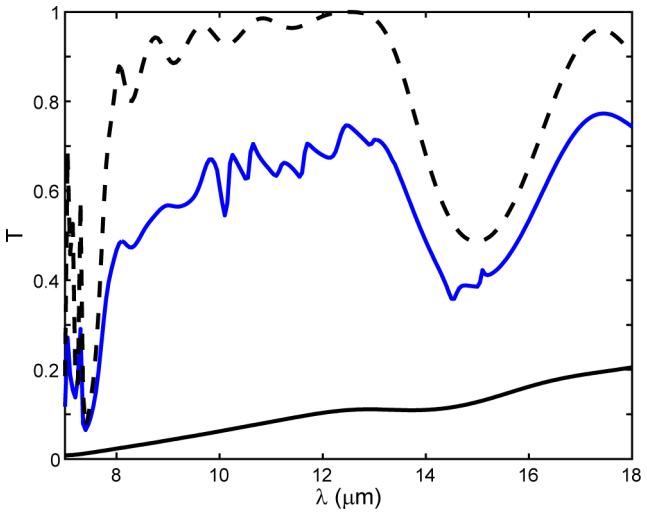

Figure 3. Normal incidence transmission spectra for textile designs based on the geometry shown in Figure 2. The black lines represent the unpolarized transmission for cotton- (solid, Figure 2a) and nylon-only (dashed, Figure 2c) fiber designs. The blue line shows the transmission for a cotton−nylon blended fiber design (Figure 2b).

for these six-layer textile designs. The black lines represent the unpolarized transmission spectrum (arithmetic average of the computed p- and s-polarized transmission spectra) for the design based on cotton fibers only (solid, Figure 2a) and for the design based on nylon fibers only (dashed, Figure 2c). The solid blue line shows the transmission spectrum for our IR transparent design based on a fiber blending scheme with nylon and cotton fibers (Figure 2b). For the cotton-only design, the transmission values are low with an average ∼0.1. For our cotton−nylon design, on the other hand, the transmission values are much larger with an average ∼0.6, which is comparable to the transmission (∼0.8 average) for the design composed of IR transparent nylon fibers only. These spectra confirm that our approach for designing photonic structure textiles has the potential for enabling textile designs that are more IR transparent than conventional textiles based purely on natural fibers (cotton) and increase transparency toward levels obtained with textiles based on IR transparent fibers only.

Any design that achieves IR transparency for increased radiative cooling should also retain opacity in the visible wavelength range. We verify this here by calculating the direct transmission through the photonic structure based on our blended cotton−nylon design. Figure 4 shows the transmission

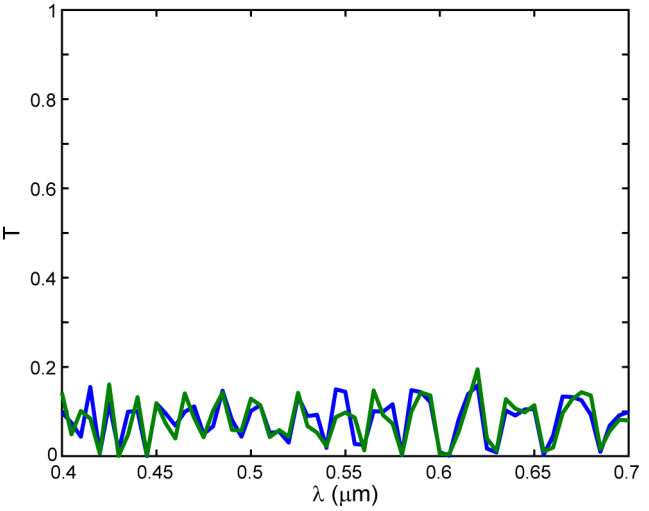

Figure 4. Direct transmission spectra at visible wavelengths (400−700 nm) for the six-layer cotton−nylon blended textile design shown in Figure 2b. The solid lines represent the p- (blue) and s-polarized (green) 0th-order transmission.

spectra in the visible wavelength range between 400 and 700 nm for normal incidence for the six-layer cotton−nylon blended textile design shown in Figure 2b. The solid lines represent the p- (blue) and s-polarized (green) transmission (0th-order only). For both polarizations, the transmission values are very small (<0.1), which means that only a very small fraction of the incident light is transmitted directly through the structure. The majority of the light is either reflected or scattered, which renders the structure opaque in the visible spectrum.

The previous calculations showed the IR spectral transmissivity for normal incidence ($\theta = 0$, $\phi = 0$) only. While fibers in textiles may not be exactly periodic over large areas, they do consist of areas that are locally periodic. Each of these areas needs to be treated properly. To account for the correct transmissivity across the full hemisphere, we now calculate spectra for all angles of incidence $\theta = 0 \rightarrow \pi/2$ and $\phi = 0 \rightarrow 2\pi$. In the discussion below, we also provide the spectrally (Planck distribution at skin temperature) and directionally weighted average of the (θ,ϕ,λ) data sets. Figure 5 shows spectral, directional transmissivity $\tau(\theta,\phi,\lambda)$ values for the cotton-only (a), cotton−nylon blended (b), and nylon-only (c) designs. Each panel show the transmissivity for incidence angles $\theta = 0 \rightarrow \pi/2$, $\phi = 0 \rightarrow 2\pi$, and IR wavelengths $\lambda = 7 \rightarrow 18\ \mu$m. The values are plotted on a coarser sampling grid for display purposes. The transmissivity of the cotton-only design varies with angle of incidence and wavelength, but remains small across the full hemisphere (∼0.06 spectrally and angularly

DOI: 10.1021/acsphotonics.6b00644
ACS Photonics XXXX, XXX, XXX−XXX

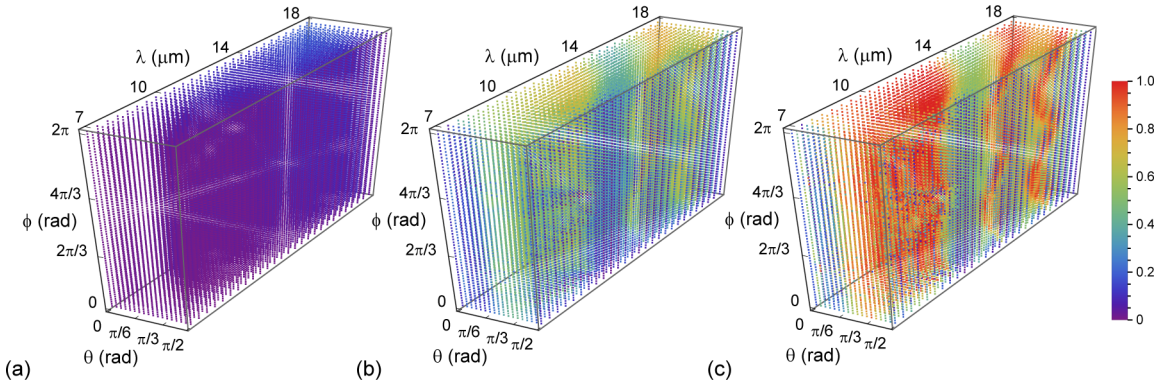

Figure 5. Spectral, directional transmissivity of cotton-only, cotton−nylon blended, and nylon-only designs. (a) Spectral, directional transmissivity $\tau(\theta,\phi,\lambda)$ of the cotton-only design (Figure 2a) for incidence angles $\theta = 0 \rightarrow \pi/2$ and $\phi = 0 \rightarrow 2\pi$, and infrared wavelengths $\lambda = 7 \rightarrow 18$ μm. (b) Spectral, directional transmissivity $\tau(\theta,\phi,\lambda)$ of the cotton−nylon design (Figure 2b) for the same range of incidence angles and wavelengths. (c) Spectral, directional transmissivity $\tau(\theta,\phi,\lambda)$ of the nylon design (Figure 2c) for the same range of incidence angles and wavelengths.

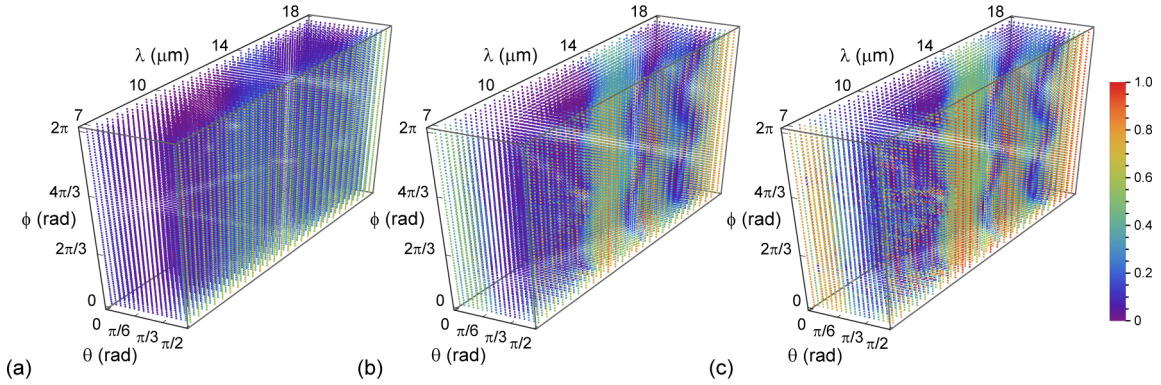

Figure 6. Spectral, directional reflectivity of cotton-only, cotton−nylon blended, and nylon-only designs. (a) Spectral, directional reflectivity $\rho(\theta,\phi,\lambda)$ of the cotton-only design (Figure 2a) for $\theta = 0 \rightarrow \pi/2$, $\phi = 0 \rightarrow 2\pi$, and $\lambda = 7 \rightarrow 18$ μm. (b) Spectral, directional reflectivity $\rho(\theta,\phi,\lambda)$ of the cotton−nylon design (Figure 2b) for the same range of incidence angles and wavelengths. (c) Spectral, directional reflectivity $\rho(\theta,\phi,\lambda)$ of the nylon-only design (Figure 2c) for the same range of incidence angles and wavelengths.

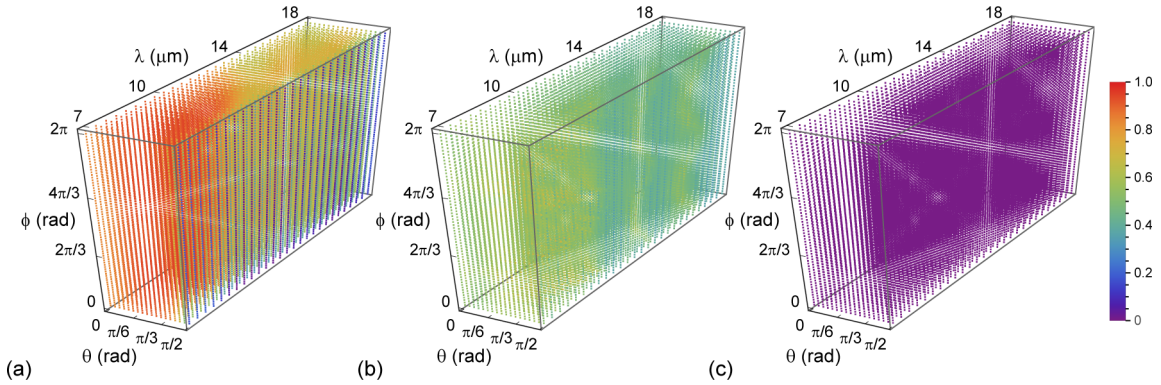

Figure 7. Spectral, directional absorptivity of cotton-only, cotton−nylon blended, and nylon-only designs. (a) Spectral, directional absorptivity $\alpha(\theta,\phi,\lambda)$ of the cotton-only design (Figure 2a) for $\theta = 0 \rightarrow \pi/2$, $\phi = 0 \rightarrow 2\pi$, and $\lambda = 7 \rightarrow 18$ μm. (b) Spectral, directional absorptivity $\alpha(\theta,\phi,\lambda)$ of the cotton−nylon design (Figure 2b) for the same range of incidence angles and wavelengths. (c) Spectral, directional absorptivity $\alpha(\theta,\phi,\lambda)$ of the nylon-only design (Figure 2c) for the same range of incidence angles and wavelengths.

weighted average). The transmissivity of the cotton−nylon design also varies with angle of incidence and wavelength, but is much larger across most of the hemisphere (~0.63 spectrally and angularly weighted average).

Figure 6 shows spectral, directional reflectivity $\rho(\theta,\phi,\lambda)$ values for the cotton-only (a), cotton−nylon blended (b), and nylon-only (c) designs. Each panel shows the reflectivity for $\theta = 0 \rightarrow \pi/2$, $\phi = 0 \rightarrow 2\pi$, and $\lambda = 7 \rightarrow 18$ μm. The reflectivity of the cotton-only design is small (~0.09 spectrally and angularly weighted average) except for angles close to grazing incidence ($\theta \approx \pi/2$). The reflectivity of the cotton−nylon design is small across the entire hemisphere as well (~0.16 spectrally and angularly weighted average), except again for angles close to grazing incidence ($\theta \approx \pi/2$).

Figure 7 shows the spectral, directional absorptivity $\alpha(\theta,\phi,\lambda)$ values for the cotton-only (a), cotton−nylon blended (b), and

DOI: 10.1021/acsphotonics.6b00644
ACS Photonics XXXX, XXX, XXX−XXX

nylon-only (c) designs. Absorptivity is calculated from transmissivity and reflectivity as $\alpha(\theta,\phi,\lambda) = 1 - \tau(\theta,\phi,\lambda) - \rho(\theta,\phi,\lambda)$. Each panel shows the reflectivity for $\theta = 0 \rightarrow \pi/2$, $\phi = 0 \rightarrow 2\pi$, and $\lambda = 7 \rightarrow 18$ μm. Absorptivity of the cotton design varies with angle of incidence and wavelength, but remains large across the entire hemisphere. The results confirm that a cotton-only-based design absorbs most of the thermal radiation between 7 and 18 μm (~0.84 spectrally and angularly weighted average). The absorptivity of the cotton–nylon design remains small across the hemisphere with a weighted average ~0.20. These full-field simulation results confirm that a cotton–nylon blended design transmits most of the thermal radiation in the 7 to 18 μm IR wavelength range, with much smaller amounts of radiation being reflected and absorbed.

Thermal Radiation Calculation. Next, we will use the directional, spectral transmission and reflection properties, which were calculated and presented above for the cotton-only design and the cotton–nylon blended design, to calculate the heat transfer between human skin and the ambient office environment for each case. For this, we develop a detailed radiative heat transfer model to quantify the net heat transfer between the human body and the office environment. Our model consists of a planar geometry comprising two parallel surfaces, which represent the human skin and the ambient office environment, respectively, separated by an intermediate layer, which represents the textile (Figure 8). The skin (heat

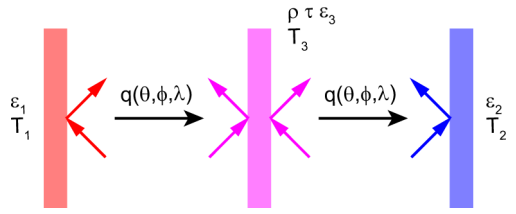

Figure 8. Geometry for radiative heat transfer between human skin (emissivity ε_1 and temperature T_1) and office wall (emissivity ε_2 and temperature T_2) separated by a semitransparent layer (transmissivity τ, reflectivity ρ, and emissivity ε_3).

source) and ambient (heat sink) are characterized by temperatures T_1 and T_2, respectively, and by emissivities ε_1 and ε_2, respectively. The intermediate (textile) layer is characterized by a transmissivity τ and a reflectivity ρ (from which emissivity ε_3 can be derived).

The standard net radiation method that is typically used to calculate the heat transfer for this one-dimensional geometry only deals with fully opaque surfaces.[24,25] This method calculates radiation heat transfer in enclosures with opaque walls.[24,26,27] It can be used to estimate the radiative heat transfer for IR opaque textiles. To calculate radiation heat transfer between opaque surfaces (skin and office wall) with a partially transparent layer (ideal, nonabsorbing textile) between them, one might use a modified net radiation method developed by Siegel.[28] This method, however, only determines the radiative heat exchange when placing an ideal, transparent layer between two parallel surfaces. To consider the effect of a semitransparent (semiabsorbing, $\varepsilon_3 \neq 0$) layer placed between two parallel surfaces (Figure 8), we further extended this method. Moreover, all these published methods typically apply to diffuse and gray surfaces. Given that transmissivity and reflectivity are typically angularly varying spectral quantities, we developed a fully directional, spectral net radiation method that takes care of these issues. The temperature of the intermediate (textile) layer (T_3) is self-consistently obtained in this method as well. The resulting directional, spectral heat flux transferred from the skin at T_1 to the office environment at T_2, is given by

$$q(\theta, \phi, \lambda) = \frac{I_{BB}(T_1, \lambda) - I_{BB}(T_2, \lambda)}{\frac{1}{\varepsilon_1(\theta,\phi,\lambda)} + \frac{1}{\varepsilon_2(\theta,\phi,\lambda)} - 2 + \frac{2}{\varepsilon_3(\theta,\phi,\lambda) + 2\tau(\theta,\phi,\lambda)}} \quad (1)$$

where $I_{BB}(T,\lambda) = (2hc^2)/(\lambda^5(e^{hc/\lambda k_B T} - 1))$ is the spectral radiance of a blackbody at temperature T, with h, c, k_B as the Planck constant, the velocity of light in vacuum, and the Boltzmann constant, respectively, and where $\varepsilon_3(\theta,\phi,\lambda) = 1 - \tau(\theta,\phi,\lambda) - \rho(\theta,\phi,\lambda)$. This is the most general expression of net spectral, directional heat flux $q(\theta,\phi,\lambda)$ and we use it below to calculate the net total radiative heat flux for the different cases.

We now calculate the net total radiative heat flux q_{tot} (W/m^2) between the human body and the office environment for a temperature set point of 23.9 °C (75 °F) at the upper end of the neutral band. We use eq 1 with the spectral, directional transmissivity and reflectivity of the cotton-only design (Figures 5a and 6a) and perform a triple integration,

$$q_{tot} = \int_{\lambda_1}^{\lambda_2} \int_{\phi=0}^{2\pi} \int_{\theta=0}^{\pi/2} q(\theta, \phi, \lambda) \cos\theta \sin\theta \, d\theta \, d\phi \, d\lambda \quad (2)$$

over the entire hemisphere and the wavelength range from $\lambda_1 = 7$ μm to $\lambda_2 = 18$ μm, which includes the peak wavelength of thermal radiation from the human body and the majority (>65%) of its emissive power. We obtain a net heat flux of 18.5 W/m^2 after summing over both polarizations. If we extend the wavelength range to between $\lambda_1 = 3$ μm and $\lambda_2 = 18$ μm, covering now more than 80% of the total blackbody emissive power, the net heat flux is 23.3 W/m^2 (after summing over both polarizations).

Next, we increase the set point from 23.9 (75) to 26.1 °C (79 °F), which is 2.2 °C (4 °F) above the thermal comfort neutral band, and again calculate the radiative heat transfer between the human body and the office ambient for the cotton design. The net heat flux reduces from 18.5 to 14.6 W/m^2 from $\lambda_1 = 7$ μm to $\lambda_2 = 18$ μm. The reduced net radiative heat transfer means that a smaller fraction of the heat generated by the human body is emitted into the office environment. This reduction in heat flow, when the ambient temperature is increased, adversely impacts thermal comfort.

Finally, we calculate the net total radiative heat flux eq 2 achieved with our blended cotton–nylon design for the office environment at 26.1 °C (79 °F). This time we use eq 1 with the spectral, directional transmissivity and reflectivity of the cotton–nylon design (Figures 5b and 6b). The resulting net heat flux is 20.2 W/m^2 in the 7–18 μm band, and 24.6 W/m^2 for the extended 3–18 μm wavelength range. In both cases, the heat transfer is beyond what is possible for the cotton-only based design for an ambient at 23.9 (75) and at 26.1 °C (79 °F). Given that these values are for the extended set point at 26.1 °C (79 °F), this means that with the cotton–nylon blended design the net heat transfer is restored to a level that is above the level necessary for thermal comfort for the cotton-only design at 23.9 °C (75 °F). Our blended cotton–nylon design thus indeed enables passive radiative cooling based on control of thermal heat transfer with photonic structure textiles.

In the six-layer design example (Figure 2b) for the calculations described above, we focused on incorporating

DOI: 10.1021/acsphotonics.6b00644
ACS Photonics XXXX, XXX, XXX–XXX

cotton fibers (~17% total cotton content) on the surface layers of the textile structure, where they matter most from a textile wearing comfort point of view. We also analyzed configurations of this six-layer design, in which an even larger fraction of cotton fibers are blended into the design. Figure 9 shows the

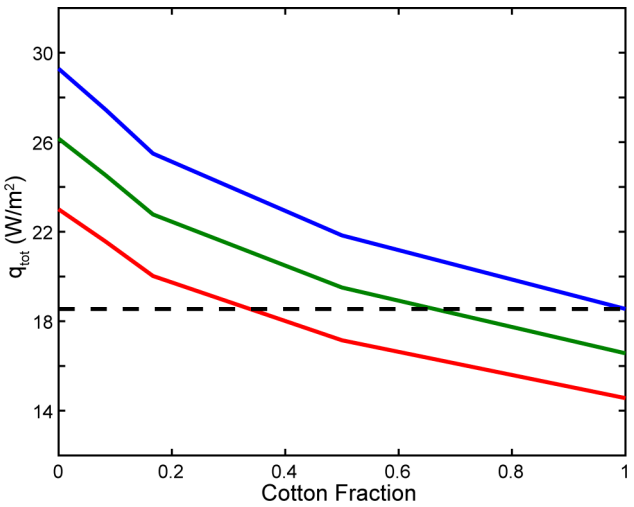

Figure 9. Outward total radiative heat flux versus cotton fraction for different ambient temperatures. The solid lines are results for the six-layer design (Figure 2) for ambient temperatures of 23.9 (75, blue), 25 (77, green), 26.1 °C (79 °F, red). The dashed black line shows the outward radiative heat flux for the reference case of a cotton-only design at an ambient temperature of 23.9 °C (75 °F).

outward total radiative heat flux (in 7−18 μm band) versus cotton fraction for different ambient temperatures. The solid lines are results for ambient temperatures of 23.9 (75, blue), 25 (77, green), and 26.1 °C (79 °F, red). The dashed black line shows the outward radiative heat flux for the case of a cotton-only design at a comfortable ambient temperature of 23.9 °C (75 °F).

It shows that a design based on our fiber blending scheme can contain as much as 34% (one-third) cotton and still perform at the extended set point of 26.1 °C (79 °F). It also shows that up to 66% (two-thirds) of cotton fibers can be blended in our design if the set point is extended by 1.1 °C (2 °F) to 25 °C (77 °F). While a set point extension by 2.2 °C (4 °F) to 26.1 °C (79 °F) can result in 12−31% energy savings, a set point extension by 1.1 °C (2 °F) still results in substantial energy savings (7−15%).

The results obtained above assume only radiative heat transfer. We now briefly consider the effects of convection (between the textile and the ambient) and heat conduction (between the skin and the textile). Assuming typical values for the air gap between skin and textile (1−5 mm) and for the convective heat transfer coefficient (3−5 W/m^2 K), we find that the combined net heat transfer for our nylon-cotton design at the extended set point of 26.1 °C (79 °F) exceeds the metabolic power rate of 58.2 W/m^2 for an adult in a sedentary state. As an additional confirmation of our approach, the combined net heat transfer for our nylon-cotton blended design at the extended set point of 26.1 °C (79 °F) also exceeds the net heat transfer at 23.9 °C (75 °F) if one assumes independently measured cotton parameters. This confirms that our approach for designing photonic structure textiles has the ability to achieve heat transfer rates that are necessary for thermal comfort at extended set points and thus can offer suitable localized thermal management for cooling.

The design principle, demonstrated here in a six-layer photonic structure prototype textile design based on commercially used fiber materials, is very generic. Any woven, knitted, or nonwoven textile design can benefit from the blending of natural and IR transparent materials, at the fiber level or at the yarn level, with the intent to render the design more IR transparent. We used cotton and nylon fibers, but our approach is not limited to these materials alone. Any conventional absorbing textile materials, including silk, linen and polyester, can be used for blending with fibers or yarns made out of IR transparent materials beyond nylon, such as for example polyethylene. The approach shown here also extends to textiles structures with more than 6 layers, where additional opportunities will exist to blend natural (IR absorbing) fibers with IR transparent fibers in order to retain the properties of natural textile fibers for comfort of wearing.

METHODS

Electromagnetic Calculations: Full Spectral, Directional Properties. We use full-vector electromagnetic (EM) field calculations, based on rigorous coupled wave analysis (RCWA),[29] to calculate the spectral, directional transmissivity $\tau(\theta,\phi,\lambda)$ and reflectivity $\rho(\theta,\phi,\lambda)$.[25] The spectral, directional emissivity $\varepsilon(\theta,\phi,\lambda)$ is derived from absorptivity $\alpha(\theta,\phi,\lambda) = 1 - \tau(\theta,\phi,\lambda) - \rho(\theta,\phi,\lambda)$ using Kirchhoff's law of thermal radiation, $\varepsilon(\theta,\phi,\lambda) = \alpha(\theta,\phi,\lambda)$. Our designs are based on cotton and nylon. For cotton, we assume a refractive index, $n_{cotton} = 1.5 + 0.1i$, in agreement with reported values.[30] We assume a refractive index $n_{nylon} = 1.6$ for nylon.[22]

Thermal Radiation Calculation. We developed a directional, spectral net radiation method to find the most general analytical expression for the spectral, directional heat flux $q(\theta,\phi,\lambda)$. The standard net radiation method that is typically used to calculate heat transfer only deals with fully opaque surfaces.[24−27] To calculate radiative heat transfer between opaque surfaces (skin and office wall) with a partially transparent layer (ideal nonabsorbing textile) between them, one might use a modified net radiation method developed by Siegel.[28] To consider the effect of a more general semi-transparent (semiabsorbing) layer and allow for a fully directional, spectral treatment, we further extended Siegel's modified method.

AUTHOR INFORMATION

Corresponding Author

*E-mail: pcatryss@stanford.edu.

ORCID

Peter B. Catrysse: 0000-0002-2389-6044

Notes

The authors declare no competing financial interest.

ACKNOWLEDGMENTS

This work is supported by the Advanced Research Projects Agency-Energy (ARPA-E), Department of Energy (Contract No. DE-AR0000533).

REFERENCES

(1) Mayernik, J. Buildings Energy Data Book. U.S. Dept. of Energy; Office of Energy Efficiency and Renewable Energy: Washington, D.C., 2012.

DOI: 10.1021/acsphotonics.6b00644
ACS Photonics XXXX, XXX, XXX−XXX

(2) Conti, J. J.; Holtberg, P. D.; Diefenderfer, J. R.; Napolitano, S. A.; Schaal, A. M.; Turnure, J. T.; Westfall, L. D. *Annual Energy Outlook 2015*; U.S. Energy Information Administration: Washington, DC, 2015.
(3) Fanger, P. O. *Thermal Comfort. Analysis and Applications in Environmental Engineering*; Danish Technical Press: Copenhagen, 1970.
(4) Hoyt, T.; Lee, K. H.; Zhang, H.; Arens, E.; Webster, T., Energy savings from extended air temperature setpoints and reductions in room air mixing. *Proceedings of the 13th International Conference on Environmental Ergonomics*, Boston, MA, 2009; Vol. *13*.
(5) ANSI/ASHRAE, *Standard 55−2013: Thermal Environmental Conditions for Human Occupancy*; ASHRAE, 2013.
(6) Law, T. *The Future of Thermal Comfort in an Energy-Constrained World*; Springer International Publishing: Cham, Switzerland, 2013.
(7) Hardy, J. D.; DuBois, E. F. Regulation of heat loss from the human body. *Proc. Natl. Acad. Sci. U. S. A.* **1937**, *23*, 624−631.
(8) Winslow, C. E. A.; Gagge, A. P.; Herrington, L. P. The influence of air movement upon heat losses from the clothed human body. *Am. J. Physiol.* **1939**, *127*, 505−518.
(9) deDear, R. J.; Arens, E.; Hui, Z.; Oguro, M. Convective and radiative heat transfer coefficients for individual human body segments. *Int. J. Biometeorol.* **1997**, *40*, 141−156.
(10) Raman, A. P.; Anoma, M. A.; Zhu, L.; Rephaeli, E.; Fan, S. Passive radiative cooling below ambient air temperature under direct sunlight. *Nature* **2014**, *515*, 540−4.
(11) Shi, N. N.; Tsai, C. C.; Camino, F.; Bernard, G. D.; Yu, N. F.; Wehner, R. Keeping cool: Enhanced optical reflection and radiative heat dissipation in Saharan silver ants. *Science* **2015**, *349*, 298−301.
(12) Rephaeli, E.; Raman, A.; Fan, S. H. Ultrabroadband Photonic Structures To Achieve High-Performance Daytime Radiative Cooling. *Nano Lett.* **2013**, *13*, 1457−1461.
(13) Zhu, L. X.; Raman, A.; Fan, S. H. Color-preserving daytime radiative cooling. *Appl. Phys. Lett.* **2013**, *103*, 103.
(14) Zhu, L. X.; Raman, A. P.; Fan, S. H. Radiative cooling of solar absorbers using a visibly transparent photonic crystal thermal blackbody. *Proc. Natl. Acad. Sci. U. S. A.* **2015**, *112*, 12282−12287.
(15) Mason, M.; Coleman, I. *Study of the Surface Emissivity of Textile Farbics and Materials in the 1 to 15 μm range*; Block Engineering, Incorporated: Cambridge, MA, 1967.
(16) Tong, J. K.; Huang, X.; Boriskina, S. V.; Loomis, J.; Xu, Y.; Chen, G. Infrared-Transparent Visible-Opaque Fabrics for Wearable Personal Thermal Management. *ACS Photonics* **2015**, *2*, 769−778.
(17) Hsu, P. C.; Song, A. Y.; Catrysse, P. B.; Liu, C.; Peng, Y.; Xie, J.; Fan, S.; Cui, Y. Radiative human body cooling by nanoporous polyethylene textile. *Science* **2016**, *353*, 1019−1023.
(18) Silverstein, R. M.; Webster, F. X.; Kiemle, D. J.; Bryce, D. L. *Spectrometric Identification of Organic Compounds*, 8th ed.; Wiley: Hoboken, NJ, 2015.
(19) Stuart, B. H. *Infrared Spectroscopy Fundamentals and Applications*; John Wiley & Sons: New York, NY, 2005.
(20) Lotens, W. A.; Pieters, A. M. J. Transfer of radiative heat through clothing ensembles. *Ergonomics* **1995**, *38*, 1132−1155.
(21) Gulmine, J. V.; Janissek, P. R.; Heise, H. M.; Akcelrud, L. Polyethylene characterization by FTIR. *Polym. Test.* **2002**, *21*, 557−563.
(22) Tompkins, H. G.; Tiwald, T.; Bungay, C.; Hooper, A. E. Use of molecular vibrations to analyze very thin films with infrared ellipsometry. *J. Phys. Chem. B* **2004**, *108*, 3777−3780.
(23) Peng, B.; Ding, T. H.; Wang, P. Propagation of polarized light through textile material. *Appl. Opt.* **2012**, *51*, 6325−6334.
(24) Siegel, R.; Howell, J. R. *Thermal Radiation Heat Transfer*, 4th ed.; Taylor & Francis: New York, 2002.
(25) Modest, M. F. *Radiative Heat Transfer*, 3rd ed.; Academic Press: New York, 2013.
(26) Sparrow, E. M.; Cess, R. D. *Radiation Heat Transfer*; Brooks Pub. Co.: Belmont, CA, 1966.
(27) Hottel, H. C.; Sarofim, A. F. *Radiative Transfer*; McGraw-Hill: New York, NY, 1967.
(28) Siegel, R. Net radiation method for enclosure systems involving partially transparent walls. *N-73-28915; NASA-TN-D-7384; E-7365*; NASA: Washington, D.C., 1973.
(29) Liu, V.; Fan, S. S4: A free electromagnetic solver for layered periodic structures. *Comput. Phys. Commun.* **2012**, *183*, 2233−2244.
(30) Aslan, M.; Yamada, J.; Menguc, M. P.; Thomasson, J. A. Characterization of individual cotton fibers via light-scattering experiments. *J. Thermophys. Heat Transfer* **2003**, *17*, 442−449.

DOI: 10.1021/acsphotonics.6b00644
ACS Photonics XXXX, XXX, XXX−XXX